FAULT ROCK EVOLUTION OF LARGE THRUST SYSTEMS ON MARS. Christian Klimczak[1], Melanie B. Callihan[1], Kelsey T. Crane[1], Corbin L. Kling[1,2], and Paul K. Byrne[2]; [1]Structural Geology and Geomechanics Group, Department of Geology, University of Georgia, Athens, GA 30602 (klimczak@uga.edu), USA, [2]Planetary Research Group, Department of Marine, Earth, and Atmospheric Sciences, North Carolina State University, Raleigh, NC 27612, USA.

Thrust Faults on Mars: Evidence suggests that large thrust fault systems, with lengths greater than the thickness of the brittle lithosphere, are widespread within the southern highlands on Mars [e.g., 1, 2]. As is typical for any large-scale fault, these thrust systems likely consist of complex zones of deformation involving one or more fault planes, a zone of intensely sheared rock (the fault core [3]), and a fault damage zone surrounding the fault core. On Mars, insight into fault zone complexity and fault rock properties from field observations is limited, such that large faults are generally approximated as one large slip plane. However, knowledge of fault rocks on Mars, and how they evolve with ongoing fault growth, is critical for understanding the frictional strength and seismic behavior of faults in the Martian lithosphere.

Sub-surface thrust fault architecture, geometry, and amount of tectonic uplift resulting from cumulative slip on the faults are expressed at the surface as asymmetric ridge with one steep and one gentle slope, with a fault surface break at or near the base of that steep slope (**Figure 1a**). Several landforms possess a few thousand meters of relief and are hundreds of kilometers long [e.g., 4]—and the largest of which are underlain by thrust faults that penetrate some 30 km into the Martian lithosphere [2,5,6]. Characterizing the along-strike morphology of such landforms affords further insights into the three-dimensional shape of their fault planes and slip distributions (described below) that, when paired with idealized fault growth models, offer clues to the rock properties of the fault core and surrounding lithosphere.

Growth of Martian Thrust Faults: We previously studied the growth geometries of 20 large thrust fault-related landforms, with a total of 25 individual fault segments, by assessing the changes of topography across the length of each of the landforms [7] (**Figure 1b**). Due to low erosion rates on Mars [8], the observed fault-related topography essentially reflects the cumulative amount of accommodated offset on the faults. The observed topographic variations along the landforms [7] (**Figure 1a**) may thus be interpreted as cumulative slip distributions. Our results indicated that although there is great variability among these slip distributions, they could be characterized as either symmetric or asymmetric, with 14 showing symmetric profiles (**Figure 1b**, left panel) and six with asymmetric profiles (**Figure 1b**, right panel). Supported by our map observations [7], we interpret many of the asymmetric slip distributions to represent fault growth influenced by interactions with other nearby structures. A few examples may also show fault tip restrictions due to lithospheric barriers caused by changes in material strength from lithology or fracture density [9–10]. Symmetric slip distributions, in contrast, are indicative of fault growth that is largely unaffected by lithospheric barriers or other nearby faults [e.g., 11].

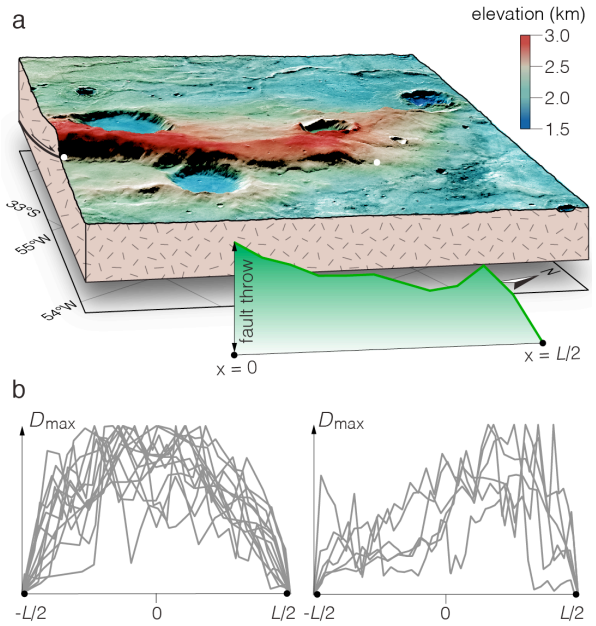

Figure 1. *Thrust fault growth on Mars. (a) Block diagram showing the northern half of Ogygis Rupes, an example of a large thrust fault-related landform on Mars. Its slip distribution is shown in the foreground. (b) Symmetric (left) and asymmetric (right) slip distributions normalized by fault length (L) and maximum displacement* (D_{max}) *of all analyzed stuctures.*

Fault Growth Models: We modeled fault growth of the 14 symmetric slip distributions with three different growth models to obtain information on fault rock properties. Fault growth was modeled by matching the measured slip distributions (**Figure 1b**) with solutions predicted by Linear Elastics Fracture Mechanics (LEFM) [12], Post-Yield Fracture Mechanics (PYFM) [12], and the Symmetric Linear Stress Distribution (SLSD) models [13] (**Figure 2a**). All growth models predict the maximum fault displacement (D_{max}) to occur in the center of the fault (at x = 0), but their overall slip distribution shapes differ insofar that the LEFM, PYFM, and SLSD models produce elliptical, bell-shaped, and peaked profiles, respectively (**Figure 2a**). All models depend on the elastic moduli of the lithosphere and, to different extents, on terms

relating frictional shear resistance and loads on the fault plane to the strength of the rock surrounding the fault plane [12,13]. Values for elastic moduli and host rock properties were adopted from previous studies [14,15]. We assumed the bulk elastic properties of the lithosphere under the Martian southern highlands to remain constant over the duration of fault growth, with no major regional variations. The best matches between our observations and model solutions were quantified as those fits that produced the lowest standard deviations (SDs). Fault rock properties for the best-fit solutions were compiled for all analyzed structures.

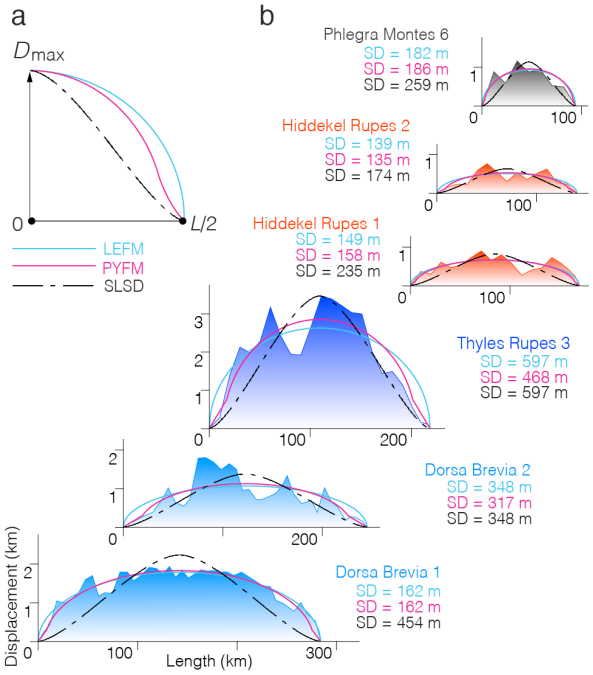

Figure 2. *Cumulative fault slip distributions. (a) Shapes of idealized symmetric fault growth models with LEFM displayed as solid blue line, PYFMshown with a solid magenta line, and SLSD with dashed black line. (b) Slip distributions of six selected thrust faults on Mars shown with best-fit solutions to the LEFM, PYFM, and SLSD models. All slip distributions are shown at the same scale with 40× vertical exaggeration. SD indicates the standard deviation between the model solution and observation.*

Fault Rock Evolution: Six selected best-fit solutions of slip distributions for each fault growth model are shown in **Figure 2b**. Overall, all models produced reasonable to very good fits with SDs much below the average displacements of the faults, but no one fault growth model was found to consistently describe the observed slip distributions better than the other two. Fault rock properties that were varied include the remote stress acting on the fault plane (for LEFM, PYFM, and SLSD) and the material strength of the host rock (for PYFM only). Both parameters represent averages over the lifetime of the faults and are related to the loading and shear strength of the fault plane and surrounding rock that are largely governed by rock friction. The best-fit solutions of *all* fault growth models return values of fault rock properties that require high remote stresses for short faults, which decrease substantially for longer faults.

Solutions to the PYFM model indicate yield strength values of 100s of MPa, which are consistent in magnitude with predictions [12] and that also exhibit an inverse relationship with fault length. This behavior implies a decrease in stress drop (as averaged over the lifetime of the faults) with increase in fault length. We hypothesize that this behavior arises from the faulting of competent country rock that is initially frictionally unstable, promotiong stick-slip conditions, but that evolves toward stable slip as wear on fault surfaces produces fault gouge with further accumulation of displacement. Information collected from model solutions on the loading conditions and fault slip will inform future calculations of the size of the zone of fault gouge surrounding the faults [16].

Conclusion: Matching slip distributions of large thrust faults in the Martian highlands with solutions for idealized fault growth models yields insight into the evolution of fault loading conditions and rock-mechanical properties at the fault. Our results point to decreases in loading and stress drops with increasing fault length, which implies that seismic behavior and frictional strength of thrust faults on Mars may have evolved as a function of accumulated offset. This behavior has been proposed from laboratory experiments [17] and is inferred from fault populations on Earth [e.g., 18].

References: [1] Watters, T. R. (1993) *JGR, 98,* 17049–17060. [2] Egea-González, I. et al. (2017) *Icarus, 288,* 53–68. [3] Caine, J. S. et al. (1996) *Geology, 24,* 1025–1028. [4] Kling, C. L. and Klimczak, C. (2016) *LPS XLVII,* Abstract #2888. [5] Schultz, R. A., and Watters, T. R. (2001) *GRL, 28,* 4659–4662. [6] Mueller, K. et al. (2014) *EPSL, 408,* 100–109. [7] Kling, C. L. (2016) *M. S. thesis, UGA,* pp. 99. [8] Golombek, M.P. and Bridges, N. T. (2000) *JGR, 105,* 1841–1853. [9] Manighetti, I. et al. (2001) *JGR, 106,* 13667–13696. [10] Davis, K. et al. (2005) *JSG, 27,* 1528–1546. [11] Nicol, A. et al. (1996) *JSG, 18,* 235–248. [12] Cowie, P. A. and Scholz, C. H. (1992) *JSG, 14,* 1133–1148. [13] Bürgmann, R. et al. (1994) *JSG, 16,* 1675–1690. [14] Schultz, R. A. et al. (2006), *JSG, 28,* 2182−2193. [15] Klimczak, C. (2015) *JGR, 120,* 2135–2151. [16] Scholz, C. H. (1987) *Geology, 15,* 493−495. [17] Ikari M. J. et al. (2011) *Geology, 39,* 83−86. [18] Wesnousky, S. G. (1990) *BSSA, 80,* 1374−1381.